AD-A085 568   ROME AIR DEVELOPMENT CENTER GRIFFISS AFB NY   F/G 17/9
                ANTENNA TECHNOLOGY FOR SPACE BASED RADAR. PART I. SUBARRAYING F--ETC(U)
                FEB 80   R J MAILLOUX
UNCLASSIFIED   RADC-TR-79-358   NL

END
DATE
FILMED
7-80
DTIC

Unclassified

REPORT DOCUMENTATION PAGE		READ INSTRUCTIONS BEFORE COMPLETING FORM
1. REPORT NUMBER RADC-TR-79-358	2. GOVT ACCESSION NO. AD-A085 568	3. RECIPIENT'S CATALOG NUMBER
4. TITLE (and Subtitle) ANTENNA TECHNOLOGY FOR SPACE BASED RADAR, PART I. SUBARRAYING FEEDS: BANDWIDTH, LOW SIDELOBE PERFORMANCE AND SUBARRAY NULLING		5. TYPE OF REPORT & PERIOD COVERED In House
		6. PERFORMING ORG. REPORT NUMBER
7. AUTHOR(s) Robert J. Mailloux		8. CONTRACT OR GRANT NUMBER(s)
9. PERFORMING ORGANIZATION NAME AND ADDRESS Deputy for Electronic Technology (RADC/EEA) Hanscom AFB Massachusetts 01731		10. PROGRAM ELEMENT, PROJECT, TASK AREA & WORK UNIT NUMBERS 62702F 4600 401
11. CONTROLLING OFFICE NAME AND ADDRESS Deputy for Electronic Technology (RADC/EEA) Hanscom AFB Massachusetts 01731		12. REPORT DATE February 1980
		13. NUMBER OF PAGES 17
14. MONITORING AGENCY NAME & ADDRESS(if different from Controlling Office)		15. SECURITY CLASS. (of this report) Unclassified
		15a. DECLASSIFICATION/DOWNGRADING SCHEDULE

16. DISTRIBUTION STATEMENT (of this Report)

Approved for public release; distribution unlimited.

17. DISTRIBUTION STATEMENT (of the abstract entered in Block 20, if different from Report)

18. SUPPLEMENTARY NOTES

19. KEY WORDS (Continue on reverse side if necessary and identify by block number)
Antenna
Phased array
Subarrays
Low sidelobe arrays

20. ABSTRACT (Continue on reverse side if necessary and identify by block number)
This brief analysis outlines the features of a subarraying system with amplitude control circuits at the feed array face. The analysis treats the idealization of the lens feed as a continuous aperture, and includes the assumption that the cylindrical lens back face is in the far field of the array feed. The analysis includes the effect of truncation at the main array, and demonstrates that the high sidelobes of the conventional $\sin x/x$ subarray illumination, when truncated, are primary contributors to high grating lobe levels under certain circumstances. The proposed correction for these

DD FORM 1473 EDITION OF 1 NOV 65 IS OBSOLETE

Unclassified

20. Abstract (Continued)

truncation effects is to produce a low sidelobe subarray illumination at the main aperture by controlling the feed array taper. Numerical results show the effectiveness of this subarraying technique for controlling the array far sidelobes and grating lobe levels, and for producing wide band null troughs within the subarray pattern.

Contents

Illustrations

3

Antenna Technology for Space Based Radar Part I. Subarraying Feeds: Bandwidth, Low Sidelobe Performance and Subarray Nulling

1. INTRODUCTION

Future space-based and ground radar systems will require wideband scanning arrays with sidelobes below -40 dB, steered nulls, and other forms of active pattern control. Since the cost of a fully time-delay steered array is prohibitive for many of these applications, there is a need for subarraying feeds so that time-delay and/or null steering can be controlled at the relatively fewer subarray inputs, while the main aperture need only have conventional phase shifters. Tang[1] described a number of subarraying feeds with varying degrees of "overlap" and using constrained or space-fed geometries. The feed system referred to by Tang as "completely overlapped" is investigated in this paper to determine its suitability for forming very low sidelobe scanned patterns and for producing nulls in the subarray pattern.

2. RADIATION CHARACTERISTICS OF THE SYSTEM

Figure 1 shows the basic configuration[1] using a one-dimensional circular lens and fixed time delays at the hybrid matrix output for subarray collimation. This

1. Tang, R. (1972) Survey of time delay beam steering techniques in phased array antennas, in Proceedings of the 1970 Phased Array Antenna Symposium, Artech House, Inc., Dedham, MA, pp 254-260.

Figure 1. Subarraying Feed for Phase Scanned Lens

specific implementation was proposed by Borgiotti[2] for a similar subarraying
system that scanned over a limited spatial sector. The main array has phase
shifters to produce a phase tilt that scans the subarray patterns. The feed is a
Fourier transformer in the form of a hybrid matrix or multiple beam lens, but
for the purposes of this analysis a multiple beam lens with true time delay will
be assumed. In addition, the feed array and the lens' faces will be modeled as
continuous apertures, and the projection factor $\cos \theta$ will be suppressed for con-
venience.

The purpose of the multiple beam feed is to form a group of N-equally spaced
illumination functions across the main array, one corresponding to each beam of
the multiple beam feed. Assuming an even number of subarray input ports to the
feed matrix, the geometry is selected so that after proper adjustments for col-
limation each beam (p) of the feed radiates to produce an illumination $g(\eta - q)$ at
the input to the phase shifters at the radiating face of the circular lens, where

$$\eta = x/D$$

2. Borgiotti, G. V. (1977) An antenna for limited scan in one plane: design
   criteria and numerical simulation, IEEE Trans. AP-25:232-243.

6

$$q = p - 1/2 \ ,$$

and D is the distance between each subarray center measured at the front lens face.

The phase shifters at the front of the lens are set to form a progressive phase tilt that is a discrete sampling of the continuous function:

$$- 2\pi \left(\frac{x}{\lambda_o} \sin \theta_o \right) \ .$$

The radiation pattern corresponding to each of the phase-shifted subarray illuminations is called the subarray pattern and is given by the following expression (after removing the relative phase displacement $2\pi q D/\lambda_o \sin \theta_o$ at the p-th subarray):

$$f(p) = \frac{1}{K} \int_{-\ell/2}^{\ell/2} e^{j2\pi(\eta-q)\beta_a} g(\eta - q) \, d\eta \qquad (1)$$

for

$$\beta_a = R S - S_o \ ,$$
$$\ell = L/D \ ,$$
$$S = (D/\lambda_o) \sin \theta \ ,$$
$$S_o = (D/\lambda_o) \sin \theta_o \ ,$$
$$R = \lambda_o/\lambda$$

and

$$K = \text{normalizing factor}.$$

Adding time-delay elements at the input of each subarray port to provide time delay corresponding to the distance $Dq \sin \theta_c$ for collimation at some angle θ_c (which may or may not correspond to the angle of the center frequency subarray beam center θ_o) results in radiation characteristics for the complete array, as given by:

$$F(S) = \sum_{p=\frac{-N}{2}+1}^{\frac{N}{2}} I_p \, f(p) \, e^{j2\pi qR(S-S_c)} \ . \qquad (2)$$

7

The array pattern is the weighted sum of the subarray patterns. If the spacing D is more than half a wavelength, the resulting pattern will have grating lobes at angles θ given by:

$$\sin \theta = \sin \theta_c + n \frac{\lambda}{D} \quad . \tag{3}$$

In the limiting case when all subarray patterns are the same, the array radiation pattern is the product of the subarray pattern and the array factor, so the grating lobe amplitude increases with the subarray sidelobe.

Thus the tapered distribution Ip controls the level of the near sidelobes (within the subarray pattern), and the subarray sidelobes control the level of the far sidelobes, because these are the grating lobes of the array factor.

The array pattern F(s) is time-delay scanned and does not squint (the peak is always at $\sin \theta = \sin \theta_c$), but the subarray pattern is a function of $(RS - S_o)$ and squints with frequency, as indicated schematically in Figure 1. For this reason, the previous developments,[1] have emphasized the formation of pulse-shaped subarray patterns to provide grating lobe suppression over a given band of frequencies. Such patterns are formed by an orthogonal hybrid network or lens with equal amplitude output coefficients. A signal applied to one of the input ports excites a set of uniformally illuminated output signals corresponding to one of the multiple beams.

The feed array excites the main array with an illumination given approximately by

$$g(\eta - q) = \sin \pi (\eta - q)/\pi (\eta - q) \quad . \tag{4}$$

If l were infinite, this excitation would produce a flat-topped pattern f(p) constant for $|\beta_a| = |RS - S_o| < 1/2$ and zero for β_a outside of that region, as shown schematically in Figure 1. This pattern provides perfect grating-lobe suppression for a very large array over a frequency bandwidth of approximately $1/S_o$. Unfortunately, the truncation of this illumination function causes relatively high subarray sidelobes and, hence, can result in unacceptable grating lobe levels for certain array sizes and illumination parameters Ip.

Figure 2 shows several subarray and array patterns for an array 10 subarrays wide ($l = 10$) with the central 8 subarrays active. Since the subarray pattern is a function of the angular difference parameter $\beta_a = D/\lambda \sin \theta - D/\lambda_o \sin \theta_o$ and not a function of the scan angle $\sin \theta_o$ alone, all figures shown in this report are plotted with θ_o equal to zero, but apply equally well to scanned or unscanned subarray patterns with the $\cos \theta$ projection factor introduced appropriately. A more thorough analysis would include lens element patterns and mutual coupling effects, but that analysis is beyond the scope of this report.
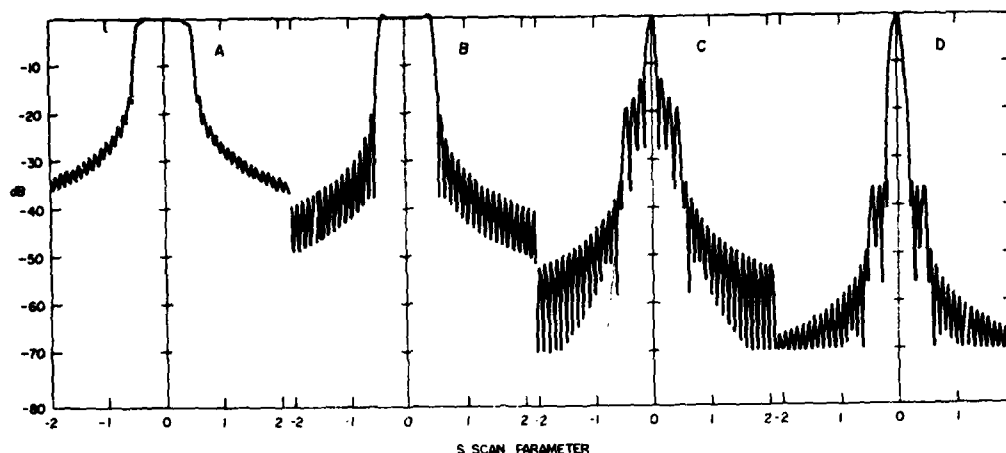
8

Figure 2. Subarray Feed With no Output Taper: A. Edge Subarray Pattern (p = -3), B. Central Subarray Pattern (p = -1), C. Radiation Pattern for Uniformally Illuminated Array, D. Radiation Pattern for Array With -35 dB Chebyshev Taper

A comparison of the subarray patterns for $p = -3$ and $p = -1$ demonstrates the deleterious effect of truncation near the array edge, and suggests the possibility of array pattern deterioration. Figure 2C shows the array radiation pattern when the subarrays are excited uniformly $\{Ip\} = 1$ and indicates significant suppression outside of the subarray angular passband, but it also shows the radiation in the grating lobe regions to be much larger than -50 dB, and so not compatible with truly low sidelobe performance. Figure 2D shows that for a -35 dB Chebyshev taper the effects of edge truncation are minimal and distortion of the subarray pattern does not lead to significant radiation in the grating lobe region. One other characteristic of these subarray patterns is worthy of notice, however, and that is that the ripples within the subarray passband are very different for the various subarrays; this suggests difficulty in forming wideband nulls at the array level, because the null formed at one frequency would not be null at another frequency since the subarray patterns do not all vary together.

As an example of an alternate approach, the curves shown in Figure 3 correspond to a feed taper given by the function $c + \cos^2 (\pi y/2b)$ for $c = 0.071$. This is indeed a severe example of feed amplitude taper, and it is used here for illustrative purposes only. The subarray illumination for this familiar function has the form:

$$g(\eta - q) = \frac{\sin \pi (\eta - q)}{\pi (\eta - q)} \left[c + \frac{1}{2} \frac{1}{(1 - (\eta - q)^2)} \right] \quad . \tag{5}$$
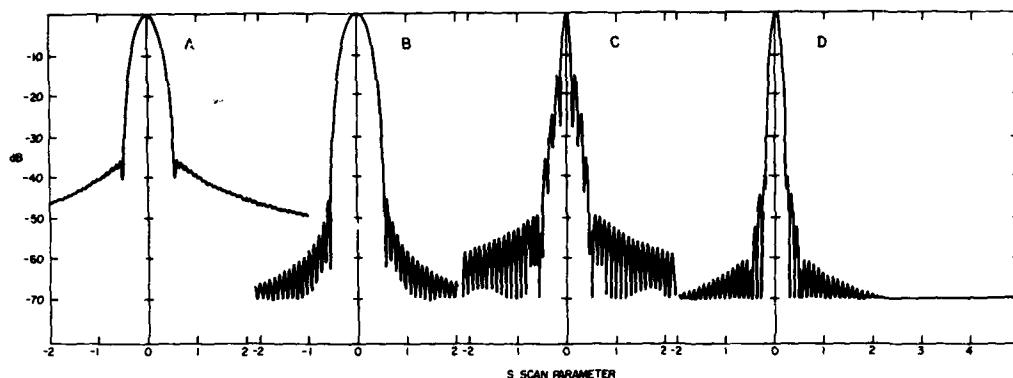
9

Figure 3. Subarray Feed With Tapered Output: A. Edge Subarray Pattern (p = -3),
B. Central Subarray Pattern (p = -1), C. Radiation Pattern for Uniformally il-
luminated Array, D. Radiation Pattern for Array With -35 dB Chebyshev Taper

This illumination has such low sidelobes that its radiation pattern is essen-
tially unaltered by truncation and has the same form as the feed taper (in the ang-
ular coordinate "S") because both the feed network illumination and the radiation
pattern are obtained by taking the Fourier transform of the subarray illumination.
Figure 3 shows this subarray pattern to have extremely low sidelobes but inferior
bandpass characteristics as compared with orthogonal subarrays. In addition,
the non-orthogonal nature of the feed distribution will introduce significant losses
in the multiple beam network; therefore, system efficiency may dictate the use of
linear amplifiers at the subarray feed. However, the use of this distribution
illustrates the possibility of producing excellent grating lobe control with low side-
lobe subarray patterns even for truncated subarray illuminations, as indicated by
comparing Figures 3A and B. Figures 3C and D show that one can obtain excellent
grating lobe control with an eight-element array of these subarrays with uniform
or -35 dB Chebychev illumination. Moreover, within the angular passband, the
subarray radiation patterns are so similar across the array that wideband null
steering is possible at the array level by using algorithms for null steering at the
array terminals (subarray ports).

In addition to array level null steering, control of the feed taper provides a
mechanism for creating nulls in the subarray pattern. At first glance it would
seem that simply forcing the feed array excitation to be zero over an extended
part of the feed would produce a subarray pattern with a wide nulled area. Figure 4
shows the subarray pattern that results from the use of a feed illumination given
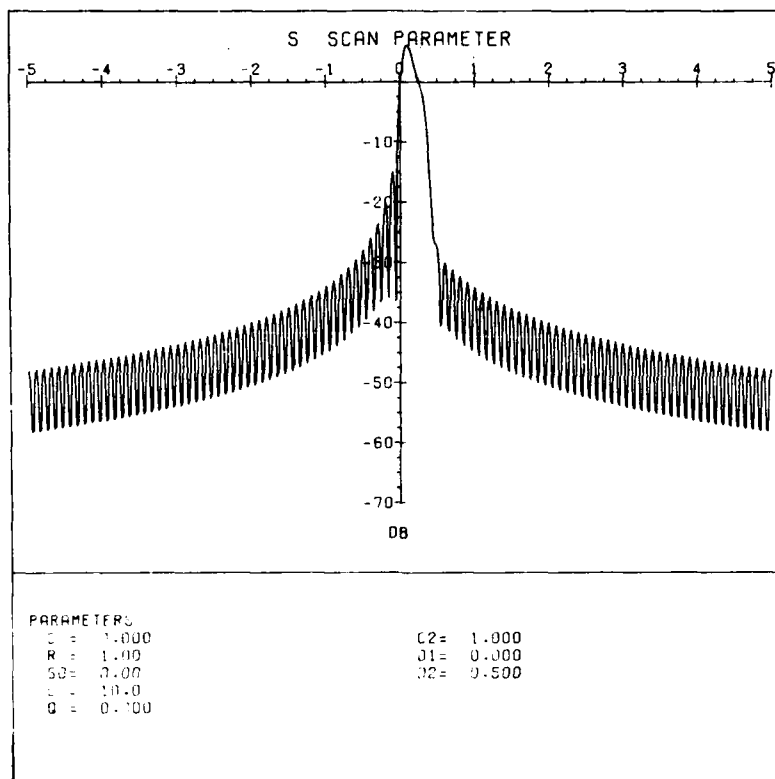by:

10

Figure 4. Subarray Pattern for the Truncated Distribution of Eq. (12)

$$a(y) = c + \cos^2 \frac{\pi y}{2b} \qquad \text{for} \qquad -b < y < 0$$

$$= 0 \qquad\qquad\quad \text{for} \qquad 0 < y < b \quad .$$

Such an illumination is suggested by the existing dual transform relationship which states that in the absence of truncation, the subarray pattern and subarray feed illumination are the same; therefore, one would expect at first that the subarray pattern of Figure 5 would have a wide trough as appropriate for wide band null formation within the subarray. Unfortunately, Figure 4 shows that this distribution suffers so severely from the effects of truncation that the trough area is filled with sidelobes.

A more successful technique for forming wide band subarray nulls follows from the use of one or several tapered illuminations instead of the discontinuous illumination above. One such feed illumination is:
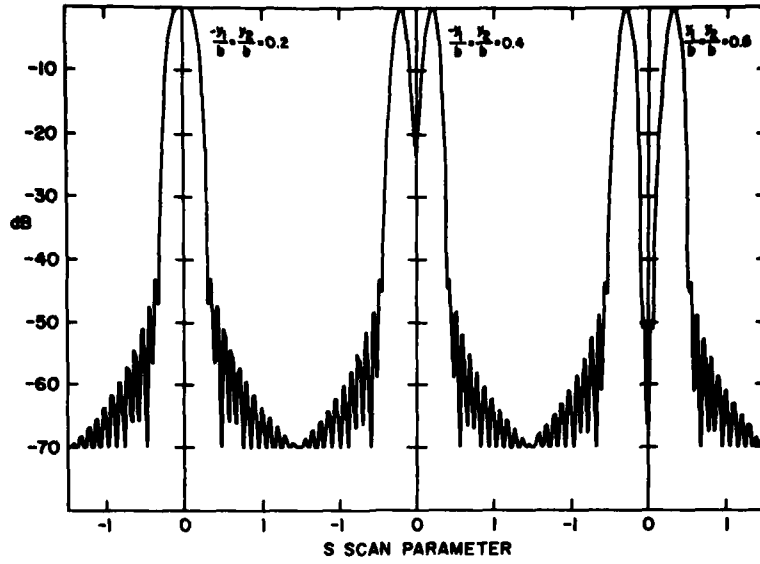
11

Figure 5. Subarray Patterns for the Illumination of Eq. (14)

$$a(y) = \left[c + \cos^2 \left(\frac{\pi(y - y_1)}{2\Delta_1} \right) \right] \quad y_1 - \Delta_1 < y < y_1 + \Delta_1$$

$$= \left[c + \cos^2 \left(\frac{\pi(y - y_2)}{2\Delta_2} \right) \right] \quad y_2 - \Delta_2 < y < y_2 + \Delta_2 \quad ,$$

(7)

and the resulting subarray illumination has the form

$$g(\eta - q) = \frac{\Delta_1}{b} e^{j\pi y_1 (\eta - q)} \left(\frac{\sin \pi[(\eta - q)\Delta_1 / b]}{\pi \frac{\Delta_1}{b}(\eta - q)} \right) \left(c + \frac{1}{2} \frac{1}{\left(1 - \left(\frac{\Delta_1}{b}\right)^2 (\eta - q)^2\right)} \right)$$

$$+ \frac{\Delta_2}{b} e^{j\pi y_2 (\eta - q)} \left(\frac{\sin \pi[(\eta - q)\Delta_2 / b]}{\pi \frac{\Delta_2}{b}(\eta - q)} \right) \left(c + \frac{1}{2} \frac{1}{\left(1 - \left(\frac{\Delta_2}{b}\right)^2 (\eta - q)^2\right)} \right).$$

(8)

12

Figure 5 shows the subarray patterns for this illumination with

$$\left(\frac{\Delta_1}{b}\right) = \left(\frac{\Delta_2}{b}\right) = 0.4 \quad ; \quad c = 0.071$$

$$l = 10$$

and

$$\frac{-y_1}{b} = \frac{y_2}{b} = 0.2 \quad , \quad 0.4 \text{ and } 0.6 \quad .$$

These curves show the resulting subarray pattern can be varied from a nearly flat-topped pattern to one with a wide trough between two peaks. The data for $-y_1 = y_2 = 0.2b$ suggests immediately that far greater bandwidth can be obtained from a flat-topped illumination with tapered edges than was achieved with the $\cos^2$ on a pedestal distribution used previously, and one might seek further optimization along these lines. As the spacing between the two illumination functions is increased to $-y_1/b = y_2/b = 0.4$ and 0.6, a null is formed over a frequency range that is proportional to the width of the trough, so the ability to control such a deep, broad trough aids substantially in wide band null control. Since $\theta_c \neq \theta_o$, it is possible to keep the subarray null fixed in position while scanning the beam over a limited sector. Alternatively, full scan capability is maintained by scanning the main beam and the subarray null.

Perhaps the most useful means of interference suppression with such a system would simply be to narrow the subarray pattern, using a tapered illumination like one of the functions in Eq. (8), or some other distribution that uses only a part of the feed array, then to use the steep skirts of the subarray pattern to discriminate against the unwanted noise signal.

In order to present a design technique for controlling the subarray pattern width in the presence of an undesired signal, it is convenient first to define the parameters determining the subarray pattern.

The main lens aperture illumination function is given by the far field expression

$$g(x) = \int_{-\infty}^{\infty} f(y) \cdot e^{jk_o y \sin\phi} dy = \int_{-\infty}^{\infty} f(y) \, e^{jk_o y (x/a)} dy \tag{9}$$

for a lens of radius a and a feed excitation f(y) defined with the region

$$-b_1 \leq y \leq b_2 \quad , \tag{10}$$

which is smaller than the full extent of the feed (Figure 2B).

The subarray far field pattern, as indicated in Eq. (1), is related to the Fourier transform of this truncated aperture illumination modified by the imposed phase shift. This dual transform relationship implies that the far field pattern of the scanned subarray is, apart from truncation effects, the same expression as the feed illumination f(y) with the parameter y replaced by the angle variable: $-a (\sin \theta - \lambda/\lambda_o \sin \theta_o)$. The subarray pattern is therefore defined within the region

$$\frac{-b_2}{a} \leq \left(\sin \theta - \frac{\lambda}{\lambda_o} \sin \theta_o \right) \leq \frac{b_1}{a} \tag{11}$$

and is essentially zero outside of that region.

The above condition results from geometric considerations of the feed. The suppression of grating lobes imposes a constraint on the size (Figure 2B) of the feed array, for, in order to obtain grating lobe suppression at a given wavelength λ for a beam at $\theta_c = \theta_o$, the width of the subarray pattern is constrained by the condition

$$-\frac{1}{2} \leq \frac{D}{\lambda} \cdot (\sin \theta - \sin \theta_o) \leq \frac{1}{2} \tag{12}$$

for inter-subarray distance D.

Using this expression and the previous one leads to the condition defining the subarray feed size at the highest frequency, assuming that the subarray width is chosen to allow scan to some maximum angle θ_{max} with S_o equal to zero. This results in the conditions

$$\frac{b}{a} \left(\frac{D}{\lambda \, min} \right) = \frac{1}{2} \quad \text{and} \quad S_{max} \leq \frac{1}{2} \frac{\lambda_{min}}{\lambda_o} \tag{13}$$

and to the final expression for the subarray width as a function of the excited fraction of the aperture:

$$- \left(\frac{\lambda_{min}}{\lambda} \right) \frac{b_2}{2b} \leq \frac{D}{\lambda} \cdot \sin \theta - \frac{D}{\lambda_o} \sin \theta_o \leq \frac{b_1}{2b} \left(\frac{\lambda_{min}}{\lambda} \right) . \tag{14}$$

14

Equation (14) can be used to derive bandwidth constraints and to determine
the optimum illuminated region of the subarray face in the presence of unwanted
noise signals. For example, as indicated in Figure 6A, if an interferring signal
radiates at an angle θ_j (in this case we assume $\theta_j > \theta_o$) and operates over a fre-
quency range bounded by the lower frequency with wavelength λ_j max and upper
frequency with λ_j min, then the system upper frequency (with wavelength λ min) is
bounded by the condition

$$\frac{D}{\lambda_{min}} \sin \theta_o \leq \frac{D}{\lambda_j \, max} \sin \theta_j \quad , \tag{15}$$

which serves to define the parameter b_1 using Eq. (14):

$$\frac{D}{\lambda_j \, max} \sin \theta_j - \frac{D}{\lambda_o} \sin \theta_o = \frac{b_1}{2b} \left(\frac{\lambda \, min}{\lambda_j \, max} \right) \quad . \tag{16}$$

This restriction ($b_1 < b$) causes the subarray pattern to be narrowed so as to
eliminate the signal at the angle of the interference in accordance with Eq. (15).
Since this example places no constraint on the lower frequency limit, the dimen-
sion b_2 can be made equal to b.

Use of Eq. (14) at the system upper and lower frequencies leads to the follow-
ing expression for system bandwidth as measured to the pattern nulls (again for a
main beam at $\sin \theta_o$):

$$BW = \frac{f \, max - f \, min}{f_o} = \left(\frac{b_1}{2bS_o} + 1 \right) \left[1 - \frac{S_o}{S_o \left(\frac{b_1}{2bS_o} + 1 \right) + \frac{b_2}{2b}} \right] \quad . \tag{17}$$

Although this analysis has been carried out assuming generalized feed illumina-
tions, the use of uniform illumination within the feed region $-b_2 \leq y \leq b_1$ will
result in unduly large truncation sidelobes, as shown in Figure 4, and the illumi-
nation throughout this region must be tapered to minimize null filling due to trun-
cation. Figure 6b shows the narrowed subarray illumination corresponding to
Eq. (8) with the parameters

$$\left(\frac{\Delta_1}{b} \right) = \left(\frac{\Delta_2}{b} \right) = 0.4 \quad , \quad \frac{y_1}{b} = +0.2 \quad , \quad \frac{y_2}{b} = +0.6 \quad , \quad l = 10 \text{ and } c = 0.071 \quad ,$$

and so gives one example of a narrowed subarray pattern with low sidelobes.
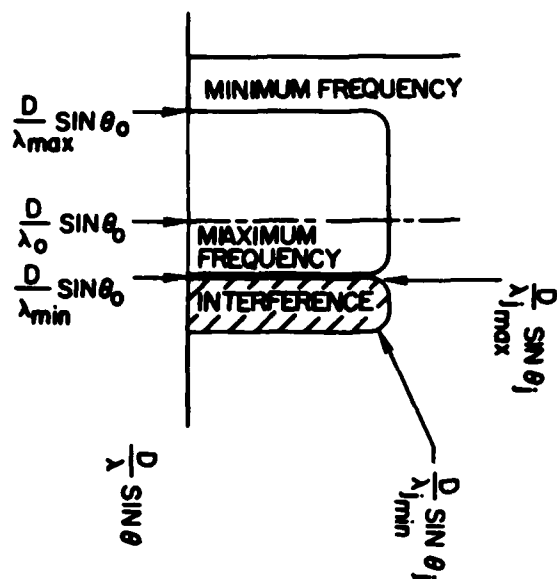
15

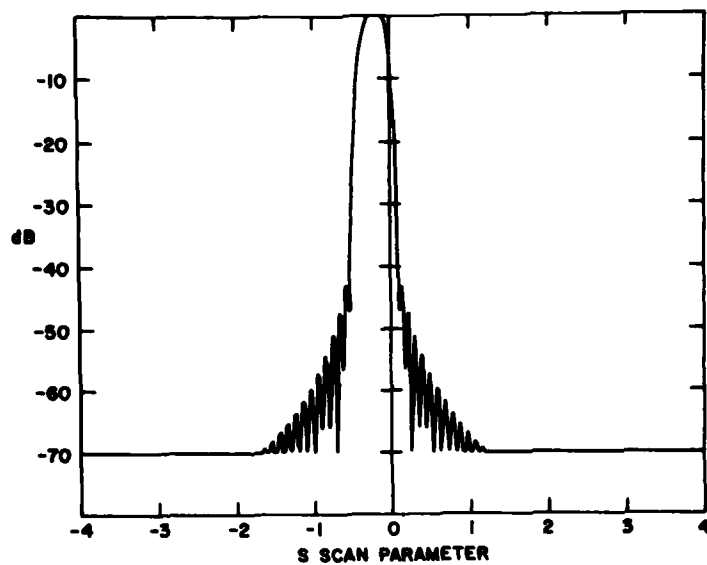Figure 6A. Narrowed Subarray for Interference Rejection

Figure 6B. Narrowed Subarray Pattern Using Eq. (8)

16

Since Eq. (17) gives bandwidth as measured to the null frequency, the actual bandwidth is less because of pattern falloff, and the use of a severely tapered illumination such as the $\cos^2 \theta$ functions used for illustrative purposes throughout this report tends to further restrict bandwidth.

Such subarray pattern control, as required to narrow the subarray pattern and avoid interfering signals, can be implemented either adaptively or deterministically. The deterministic solution can be obtained from the above equations directly, based upon knowledge of the position and bandwidth of the interfering and desired signals. The adaptive solution would differ in principle from conventional algorithms in that the adaptive weighting is applied at the subarray feed aperture and that it should discriminate on the basis of received frequency and location of the received signal on the feed aperture. Since the received signal from any one point in space is projected to different areas on the feed surface, depending upon the source frequency, then by discriminating on the basis of frequency and feed illumination the technique can accommodate null placement in the direction of any interfering source, unless it occupies the same frequency spectrum limits and angular location as the desired source.

3. CONCLUSION

This analysis has treated the case of an optically subarraying feed with amplitude control at the feed aperture. The two main conclusions are that the feed taper can result in extremely low sidelobe subarray patterns and can produce subarray troughs consistent with wideband null formation.

The increased loss resulting from use of such non-orthogonal subarray illuminations is best compensated using amplifiers at the feed aperture, but with this loss overcome the system allows a degree of control not available with other types of subarraying systems. This added control includes the ability to form low sidelobe subarray patterns for wide band performance, the formation of subarray nulls or troughs with reasonable bandwidth and good array sidelobes, and combinations of the above.

17